Rose-Hulman Institute of Technology

Rose-Hulman Scholar

Mathematical Sciences Technical Reports (MSTR)

Mathematics

7-20-2005

Time-Dependent Thermal Imaging of Circular Inclusions

Donald L. Brouwn
Rose-Hulman Institute of Technology

Mark Hubenthal
Rose-Hulman Institute of Technology

Follow this and additional works at: https://scholar.rose-hulman.edu/math_mstr

 Part of the Mathematics Commons, Numerical Analysis and Computation Commons, and the Partial Differential Equations Commons

Recommended Citation

Brouwn, Donald L. and Hubenthal, Mark, "Time-Dependent Thermal Imaging of Circular Inclusions" (2005). *Mathematical Sciences Technical Reports (MSTR)*. 50.
https://scholar.rose-hulman.edu/math_mstr/50

This Article is brought to you for free and open access by the Mathematics at Rose-Hulman Scholar. It has been accepted for inclusion in Mathematical Sciences Technical Reports (MSTR) by an authorized administrator of Rose-Hulman Scholar. For more information, please contact weir1@rose-hulman.edu.

TIME DEPENDENT THERMAL IMAGING OF CIRCULAR INCLUSIONS

Donald L. Brown and Mark Hubenthal
Advisor: Kurt Bryan

MS TR 05-02

July 20, 2005

Department of Mathematics
Rose-Hulman Institute of Technology

FAX : (812) 877-8883 **Phone: (812) 877-8391**

Time Dependent Thermal Imaging of Circular Inclusions

Donald L. Brown and Mark Hubenthal
Advisor: Dr. Kurt Bryan

July 20, 2005

Abstract

This paper considers the inverse problem of locating one or more circular inclusions in a two-dimensional domain using thermal boundary data, specifically, the input heat flux and measured boundary temperature. The forward problem is governed by the heat equation. We show how the position and size of such defects can be recovered using the boundary data of D and various approximations of the solution to the forward problem. We also consider the stability of the algorithm involved to recover the defects.

Contents

List of Figures

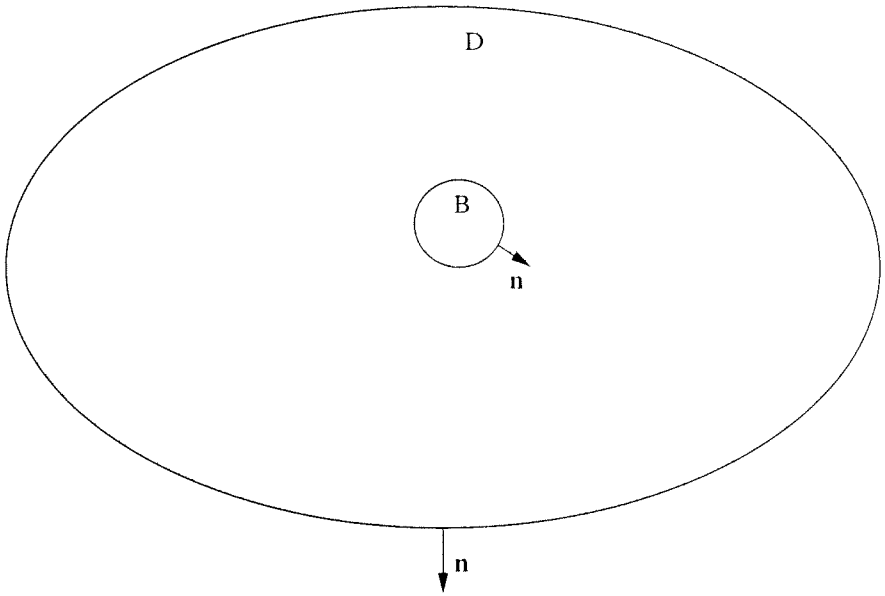

Figure 1: The Forward Problem

1 Introduction

Much research currently exists on recovering the location, size, and orientation of defects embedded in some domain, by using only data taken on the boundary of the entire region. In general, such inverse problems do not have an exact solution that we can obtain using standard methods, and so various approximations must be made. The overall goal is to develop an algorithm to recover information about the interior of the domain with minimal computation and maximal accuracy. In this paper we will consider the problem of recovering perfectly insulating circular inclusions in a given two-dimensional domain using thermal data. Previous results in related inverse problems, such as the Reciprocity Gap approach (as described in, e.g., [2]) and the Laplace Transform will be of considerable use in this paper.

2 The Forward Problem

Let D be a bounded region in $\mathbb{R}^2$ with boundary ∂D. The time dependent temperature at any point (x, y) inside of D will be denoted by the function $u(x, y, t)$. For simplicity, we will assume the diffusivity constant throughout D to be 1. The function $u(x, y, t)$ will thus obey

the time-dependent heat equation

$$\frac{\partial u}{\partial t} = \Delta u \tag{1}$$

in D. We also assume that a heat flux, g, is applied the external boundary, so that on ∂D we have

$$\frac{\partial u}{\partial \mathbf{n}} = g \tag{2}$$

where $\mathbf{n}$ is a unit outward vector normal to ∂D. We assume that the initial temperature is zero in all of D.

Now suppose that a circular inclusion B lies inside of D; we assume that B completely blocks the flow of heat. We still have that (1) holds for all $(x, y) \in D \setminus B$, but since B is perfectly-insulating, heat flow across ∂B is completely obstructed. Thus,

$$\frac{\partial u}{\partial \mathbf{n}} = 0 \text{ on } \quad \partial B \tag{3}$$

The forward problem consists of finding the solution to equations (1)-(3) (with initial condition $u(x, y, 0) = 0$) from knowledge of B. However, we are interested in extracting information about B from knowledge of the input flux g and solution u on ∂D.

3 Transforming the Heat Equation

3.1 Laplace Transform

Our first step in recovering the size and location of the inclusion B is to make use of the Laplace transform with respect to time t to eliminate that variable from the problem. Not only is this a great simplification it also allows us an extra degree of freedom.

We denote the Laplace transform of a function $f(x, y, t)$ (with respect to t) by $\mathfrak{L}[f](x, y, s)$, defined for $s \geq 0$ as

$$\mathfrak{L}[f](x, y, s) = \int_0^\infty e^{-st} f(x, y, t)\, dt \tag{4}$$

3.2 Transformed Problem

Applying the Laplace Transform to (1)-(3) and making use of the initial condition $u(x, y, 0) = 0$ yields a partial differential equation (PDE) of the form

$$sU_s - \Delta U_s = 0 \text{ in } D \setminus B \tag{5}$$

$$\frac{\partial U_s}{\partial \mathbf{n}} = G_s \text{ on } \partial D \tag{6}$$

$$\frac{\partial U_s}{\partial \mathbf{n}} = 0 \text{ on } \partial B \tag{7}$$

where $U_s(x,y) = \int_0^\infty e^{-st}u(x,y,t)\,dt$ and $G_s(x,y) = \int_0^\infty e^{-st}g(x,y,t)\,dt$. We assume here that the flux g decays sufficiently rapidly so that the relevant transforms exists for $s \geq 0$.

We will consider recovery of B in both the cases $s = 0$ and $s > 0$. For the $s = 0$ case this will distill down to what is called the Laplace equation, or equivalently, the steady state case.

4 The Steady State Case ($s = 0$)

First, note that in setting $s = 0$ we put a couple mathematical restriction on the heat flux g. If $s = 0$ then we require that g decay rapidly enough so that the integral defining $G_0(x,y)$ converges; moreover, in order that equations (5)-(6) to have a solution, we need $\int_{\partial D} G_0(x,y)\,ds = 0$. This forces the condition

$$\int_0^\infty \int_{\partial D} g(x,y,t)\,ds\,dt = 0,$$

that is, that the net heat energy input is zero. We assume this (for the case $s = 0$ only), and in fact it will be convenient to also assume that $g = 0$ for sufficiently large t These conditions ensure that the temperature u will decay to zero for sufficiently large t.

With this in mind, equations (5)-(7) become simply Laplace's Equation with Neumann boundary conditions

$$\Delta U_0 = 0 \text{ in } D \setminus B \tag{8}$$

$$\frac{\partial U_0}{\partial \mathbf{n}} = G_0(x,y) \text{ on } \partial D \tag{9}$$

$$\frac{\partial U_0}{\partial \mathbf{n}} = 0 \text{ on } \partial B \tag{10}$$

In the following sections we outline a method to recover the inclusion for the steady state case. To recover the center of B we will use the Reciprocity Gap functional.

4.1 Reciprocity Gap

The Reciprocity Gap functional will allow us to obtain information about the inclusion B from the thermal measurements on the boundary ∂D. To derive the Reciprocity Gap we will apply Green's second identity to the functions U_0 and a "test function" $w \in C^2(\bar{D})$. First recall the following theorem ([4]).

Theorem 1 (Green's Second Identity) *For any pair of functions f and g that are $C^2(\overline{D})$,*

$$\int\int_D (f\Delta g - g\Delta f)\,dA = \int_{\partial D} \left(f\frac{\partial g}{\partial \mathbf{n}} - g\frac{\partial f}{\partial \mathbf{n}} \right) ds.$$

Let w be a function which is in $C^2(\bar{D})$. Applying Green's second identity to U_0 and w on the domain $D \setminus B$ yields

$$\int_{D\setminus B} (U_0 \Delta w - w \Delta U_0)\, dA = \int_{\partial D \cup \partial B} \left(U_0 \frac{\partial w}{\partial \mathbf{n}} - w \frac{\partial U_0}{\partial \mathbf{n}} \right) ds.$$

Since both U_0 and w are harmonic, the left side above is zero. We split the boundary integral on the right (note that $\mathbf{n}$ points out of B, hence INTO $D \setminus B$) and obtain

$$\mathrm{RG}(w) := \int_{\partial D} \left(U_0 \frac{\partial w}{\partial \mathbf{n}} - w \frac{\partial U_0}{\partial \mathbf{n}} \right) ds = \int_{\partial B} U_0 \frac{\partial w}{\partial \mathbf{n}}\, ds \tag{11}$$

We use $RG(w)$ as a shorthand for the left side of equation (11). Note that $RG(w)$ can be computed from knowledge of w, g, and u on ∂D for $t > 0$. The goal now is to use cleverly chosen test functions w in equation (11) to extract information about B.

4.2 The Test Functions

Let η be any non-zero complex number. We use the following class of test functions and their derivatives with respect to η in the $s = 0$ case:

$$w = \frac{e^{\eta(x+iy)}}{\eta} \tag{12}$$

$$\frac{\partial w}{\partial \eta} = \frac{x+iy}{\eta} e^{\eta(x+iy)} \tag{13}$$

If we parameterize ∂B for $\theta \in [0, 2\pi)$ as $x = x^* + R\cos(\theta), y = y^* + R\sin(\theta)$ (where (x^*, y^*) is the center of B and R is the radius of B) then we find $\mathbf{n} =< \cos\theta, \sin\theta >$ and we compute $\frac{\partial w}{\partial \mathbf{n}}$ on ∂B as

$$\begin{aligned} \frac{\partial w}{\partial \mathbf{n}} &= \nabla w \cdot \mathbf{n} \\ &= < e^{\eta(x+iy)}, ie^{\eta(x+iy)} > \cdot < \cos(\theta), \sin(\theta) > \\ &= e^{i\theta} e^{\eta(x+iy)} \\ &= e^{i\theta} e^{\eta z^*} e^{\eta R e^{i\theta}} \end{aligned} \tag{14}$$

where $z^* = x^* + iy^*$.

4.3 Finding the Center of a Single Inclusion

Let us consider $RG(w)$ as a function of η, and write $\phi(\eta) = RG(w)$ with w chosen according to equation (12). We can use equation (14) to find that

$$\phi(\eta) = e^{\eta z^*} \int_{\partial B} e^{i\theta} e^{\eta R e^{i\theta}} U_0(\theta)\, ds \tag{15}$$

where we write $U_0(\theta) = U_0(x^* + R\cos(\theta), y^* + R\sin(\theta))$.

Let us assume that R is small, and approximate $e^{\eta R i\theta}$ as $1+O(\eta R)$, where $O(\eta R)$ denotes a quantity bounded in magnitude by $A|\eta R|$, where A is independent of η and R. We then find that we can approximate

$$\phi(\eta) \approx e^{\eta z^*} \int_{\partial B} e^{i\theta} U_0(\theta)\, ds \tag{16}$$

where the terms that have been dropped are (at least) one order of R higher, so the approximation should improve as R gets closer to zero.

Now, because $\frac{\partial w}{\partial \eta}$ is also harmonic with w taken from (12), we can similarly compute that $\phi'(\eta) = \mathrm{RG}(\frac{\partial w}{\partial \eta})$ (this is computable from the boundary data on D). We then have

$$z^* = \frac{\phi'(\eta)}{\phi(\eta)} = \frac{RG(w)}{RG(\partial w/\partial \eta)} \tag{17}$$

for any non-zero complex η. Thus we can recover the center of B. An example is provided below in section 4.5.

4.4 Finding the Radius of a Single Inclusion for $s = 0$

The above procedure also recovers (approximately) the value of the integral $\int_{\partial B} e^{i\theta} U_0(\theta)\, ds$. In the following section we derive a relation between this integral and R, the radius of the inclusion.

4.4.1 Approximate Solution to (8)-(10)

Now that we know where the center of the inclusion B is, we can assume that our coordinate system is shifted so that z^* is at the origin. We will use polar coordinates (r, θ) in what follows.

Let us write U_0 as the sum $U_0 = u_0 + v_0$, where u_0 solves equation (8) on the uncracked domain D with the Neumann boundary condition $\frac{\partial u_0}{\partial \mathbf{n}} = g$ on ∂D. The function v_0 is a perturbation of u_0 that satisfies the problem

$$\Delta v_0 = 0 \text{ on } D \setminus B \tag{18}$$

$$\frac{\partial v_0}{\partial \mathbf{n}} = 0 \text{ on } \partial D \tag{19}$$

$$\frac{\partial v_0}{\partial \mathbf{n}} = -\frac{\partial u_0}{\partial \mathbf{n}} := h(\theta) \text{ on } \partial B \tag{20}$$

We will write out a solution to the boundary value problem (18)-(20), but without the condition $\frac{\partial v_0}{\partial \mathbf{n}} = 0$ on ∂D. Rather, this condition will be "approximately" satisfied, asymptotically as R approaches zero. This turns out to be sufficiently accurate for our purposes.

It's worth noting that u_0 is computable from the input flux g, and so may be treated as a known quantity.

In what follows we will construct an approximation v to the function v_0. Our approximation v will satisfy (18) and (20), but not (exactly) equation (19). On ∂B we have $\frac{\partial}{\partial \mathbf{n}} = \frac{\partial}{\partial r}$, so equation (20) can be written

$$\frac{\partial v}{\partial r} = h(\theta). \tag{21}$$

Moreover, in polar coordinates the equation (8) becomes

$$\frac{\partial^2 v}{\partial r^2} + \frac{1}{r}\frac{\partial v}{\partial r} + \frac{1}{r^2}\frac{\partial^2 v}{\partial \theta^2} = 0 \tag{22}$$

Using separation of variables, we obtain the following two ordinary differential equations, assuming that $v(r,\theta) = \alpha(r)\beta(\theta)$.

$$\begin{aligned} \beta'' + \lambda\beta &= 0 \\ \alpha'' + \frac{1}{r}\alpha' - \frac{\lambda\alpha}{r^2} &= 0 \end{aligned}$$

We can write $v(r,\theta)$ as an infinite series of eigenfunctions $\alpha_k\beta_k$,

$$v(r,\theta) = \sum_{k=1}^{\infty} r^{-k}\left(a_k \cos(k\theta) + b_k \sin(k\theta)\right) \tag{23}$$

Here we have chosen those eigenfunctions which decay rapidly to zero as $r \to \infty$ (but are singular at $r = 0$). This will allow us to obtain the boundary condition (20) exactly, while (19) will be satisfied to "good" accuracy if R is small.

Since β must be a periodic function from the consistency condition $\beta(\theta) = \beta(\theta + 2\pi)$, it follows that λ must be positive. Letting $\sqrt{\lambda} = k$, we have

$$\begin{aligned} \beta(\theta) &= c_1 \cos(k\theta) + c_2 \sin(k\theta) \\ \alpha(r) &= c_3 r^k + c_4 r^{-k} \end{aligned}$$

Since any part of the solution with a θ dependence must repeat every 2π radians, we have that $\cos(k(\theta + 2\pi)) = \cos(k\theta)$. Thus, $2k\pi$ must be a multiple of 2π and so k is an integer. Furthermore, since we want v to be bounded far away from B, c_3 must be zero.

Differentiating equation (23) with respect to r and evaluating at $r = R$ gives (in light of equation (21))

$$\frac{\partial v}{\partial r}(R,\theta) = \sum_{k=1}^{\infty} -kR^{-(k+1)}\left(a_k \sin(k\theta) + b_k \cos(k\theta)\right) = h(\theta)$$

We can compute the coefficients a_k and b_k by viewing h as a Fourier series on the interval $0 \leq \theta \leq 2\pi$, and so find that

$$\begin{aligned} -kR^{-(k+1)}a_k &= \frac{1}{\pi}\int_0^{2\pi} h(\theta)\cos(k\theta)\,d\theta \\ -kR^{-(k+1)}b_k &= \frac{1}{\pi}\int_0^{2\pi} h(\theta)\sin(k\theta)\,d\theta. \end{aligned}$$

We obtain

$$\begin{aligned} a_k &= -\frac{R^{k+1}}{k\pi}\int_0^{2\pi} h(\theta)\cos(k\theta)\,d\theta \\ b_k &= -\frac{R^{k+1}}{k\pi}\int_0^{2\pi} h(\theta)\sin(k\theta)\,d\theta \end{aligned}$$

We then have an approximate solution v to equations (18)-(20) given by

$$v(r,\theta) = -R\sum_{k=1}^{\infty}\frac{R^k}{kr^k}\left(a'_k\cos(k\theta) + b'_k\sin(k\theta)\right) \tag{24}$$

where

$$a'_k = \frac{1}{\pi}\int_0^{2\pi} h(\theta)\cos(k\theta)\,d\theta, \quad b'_k = \frac{1}{\pi}\int_0^{2\pi} h(\theta)\sin(k\theta)\,d\theta. \tag{25}$$

For any fixed r the function v its derivatives decay rapidly to zero at $R \to 0$, so for small R equation (19) should be satisfied to increasingly good approximation (this part we have not rigorously proved).

4.4.2 The Relation of $RG(w)$ to R

Recall our definition of $\phi(\eta) = \mathrm{RG}(w)$ where w is taken from equation (12). We want to expand the expression for $\phi(\eta)$ using $U_0 \approx u_0 + v$ and a few other suitable approximations in order to derive a relation between $\phi(\eta)$ and the radius R of B. Recall that

$$\phi(\eta) := \mathrm{RG}(w) = \int_{\partial B}\frac{\partial w}{\partial \mathbf{n}}U_0\,ds. \tag{26}$$

If the defect B is relatively small then w and ∇w will be approximately constant over B. Thus, as in the computations that lead to equation (14) and making use of $R \approx 0$ we find, as before,

$$\frac{\partial w}{\partial \mathbf{n}}|_{\partial B} \approx e^{i\theta}e^{\eta z^*} + O(R)$$

with ∂B parameterized as $z^* + e^{i\theta}$. We then have from (26) that

$$\begin{aligned} \phi(\eta) &= \int_{\partial B} \frac{\partial w}{\partial \mathbf{n}} U_0 \, ds \\ &\approx e^{\eta z^*} \int_0^{2\pi} e^{i\theta} U_0(R,\theta) R \, d\theta \\ &= J e^{\eta z^*} \end{aligned} \tag{27}$$

where

$$J = \int_0^{2\pi} e^{i\theta} U_0(R,\theta) R \, d\theta \tag{28}$$

We next use the approximation $U_0 = u_0 + v$ to find

$$J \approx \int_0^{2\pi} e^{i\theta} u_0(R,\theta) R \, d\theta + \int_0^{2\pi} e^{i\theta} v(R,\theta) R \, d\theta. \tag{29}$$

We can then approximate $u_0(R,\theta)$ on ∂B by a partial Taylor expansion

$$u_0|_{\partial B} \approx u_0(z^*) + \nabla u_0(z^*) \cdot < R\cos\theta, R\sin\theta > + O(R^2) \tag{30}$$

Note that $u_0(z^*)$ is a constant and disappears when integrated against the $e^{i\theta}$ factor in (14). We have then that

$$\begin{aligned} \int_0^{2\pi} e^{i\theta} u_0(R,\theta) R \, d\theta &= \int_0^{2\pi} e^{i\theta} u_0(z^*) R \, d\theta + \int_0^{2\pi} e^{i\theta} \nabla u_0(z^*) \cdot < \cos(\theta), \sin(\theta) > R^2 \, d\theta + O(R^3) \\ &= \pi R^2 \left(\frac{\partial u_0}{\partial x}(z^*) + i \frac{\partial u_0}{\partial y}(z^*) \right) + O(R^3) \end{aligned} \tag{31}$$

Similarly, making use of equation (24) for $r = R$ and invoking the orthogonality of the trig functions yields

$$\int_0^{2\pi} e^{i\theta} v(R,\theta) R \, d\theta = -\pi R^2 (a_1' + i b_1') \tag{32}$$

with a_1' and b_1' defined by equations (25). This can be further simplified by noting that (recall equation (21)) on ∂B, $h(\theta) = -\frac{\partial u_0}{\partial r} = -\nabla u_0(R,\theta) \cdot < \cos\theta, \sin\theta > = -\nabla u_0(z^*) \cdot < \cos\theta, \sin\theta > + O(R)$. Then

$$\begin{aligned} a_1' &= -\frac{1}{\pi} \int_0^{2\pi} \left(\frac{\partial u_0}{\partial x}(z^*) \cos(\theta) + \frac{\partial u_0}{\partial y}(z^*) \sin(\theta) \right) \cos(\theta) \, d\theta + O(R) \\ &= 1 + O(R) \end{aligned}$$

and similarly $b_1' = 1 + O(R)$. From this and equations (32), (31), and (29) we find

$$J = 2\pi R^2 \left(\frac{\partial u_0}{\partial x}(z^*) + i \frac{\partial u_0}{\partial y}(z^*) \right) + O(R^3)$$

With equation (27) we have the important result

$$\phi(\eta) = 2\pi R^2 \left(\frac{\partial u_0}{\partial x}(z^*) + i \frac{\partial u_0}{\partial y}(z^*) \right) e^{\eta z^*} + O(R^3) \tag{33}$$

After dropping the $O(R^3)$ term, we can use equation (33) to estimate the radius of a single inclusion. First note that we have already shown how to estimate z^*. Also, the function u_0 is known. We may thus estimate R by taking the magnitude of both sides and solving as

$$R \approx \left(\frac{|\phi(\eta)|}{2\pi |e^{\eta z^*}| |\nabla u_0(z^*)|} \right)^{1/2}. \tag{34}$$

4.5 A Single Inclusion Example

In the following example we take D as the unit disk. The inclusion B is a disk of radius 0.2 centered at $(0.2, 0.4)$ in an xy coordinate system. The input flux used is $g(\theta, t) = \sin(\pi t)\sin(\theta)$ for $0 < t < 1$, then $g \equiv 0$. The solution to the full heat equation was computed for $0 < t < 3$ using FemLab, then integrated in time to produce the function $U_0(x, y)$.

With the choice $\eta = 1$ we obtain $\phi(1) \approx -0.0812 + 0.1934i$ and $\phi'(1) \approx -0.0934 + 0.0059i$. This yields the estimate

$$z^* = \frac{-0.0812 + 0.1934i}{-0.0934 + 0.0059i} \approx 0.1982 + 0.3998i$$

which is extremely good. Now the harmonic function u_0 corresponding to the "no inclusion" case is given by $u_0(x, y) = 2/\pi y$, and so $\nabla u_0 \equiv < 0, 2/\pi >$. Equation (34) then yields

$$R \approx \left| \frac{-0.0812 + 0.1934i}{4e^{0.1982 + 0.3998i}} \right|^{1/2} \approx 0.2074$$

which is also very good.

4.6 Identification of Multiple Inclusions

The method we used for multiple inclusions in the $s = 0$ case is adapted from the method used in [3], although it was originally used with linear cracks, thus adding the "crack angle" to the list of parameters. We use the same test function as defined in equation (12). The

reciprocity gap functional, however, is now a sum of exponentials in η. Let n be the number of circular inclusions present. Analysis similar to the single inclusion case yields

$$\phi(\eta) := \mathrm{RG}(w) \approx \sum_{j=1}^{n} e^{\eta z_j^*} \int_{\partial B_j} e^{i\theta} u(\theta)\, ds \tag{35}$$

If we define $A_j = \int_{\partial B_j} e^{i\theta} u(\theta)\, ds$ for each $1 \leq j \leq n$, we get

$$\phi(\eta) = \sum_{j=1}^{n} A_j e^{\eta z_j^*} \tag{36}$$

Very similar computations to those in the single inclusion case show that we can expect

$$A_j \;=\; 2\pi R_j^2 \left(\frac{\partial u_0}{\partial x}(z_j^*) + i \frac{\partial u_0}{\partial y}(z_j^*) \right) + O(R_j^3). \tag{37}$$

Our goal is to identity the centers z_j^*, and then each of the jump integrals A_j. Equation (37) will then allow us to estimate the radii of the inclusions (after dropping the $O(R^3)$ term) as

$$R_j \approx \left(\frac{|A_j|}{2\pi |\nabla u_0(z_j^*)|} \right)^{1/2}. \tag{38}$$

Now, because $\phi(\eta)$ and its derivatives are essentially sums of exponentials multiplied by various non-η dependent constants, we know that $\phi(\eta)$ satisfies the differential equation

$$\phi^{(n)}(\eta) + c_{n-1}\phi^{(n-1)}(\eta) + \cdots + c_1 \phi'(\eta) + c_0 \phi(\eta) = 0 \tag{39}$$

where the c_j are determined by the characteristic polynomial for the above ODE (39)

$$p(x) = \prod_{j=1}^{n} (x - z_j^*) = x^n + \sum_{j=0}^{n-1} c_j x^j \tag{40}$$

By exploiting our ability to compute the derivatives of $\phi(\eta)$, we can identify the coefficients c_j. Assuming that we don't know what n is, we'll let N be an upper bound on the number of inclusions that is chosen ahead of time, so $N \geq n$. We'll then choose complex numbers $\eta_1, \eta_2, \ldots, \eta_N$ and compute $\phi^{(j)}(\eta_k)$ for $0 \leq j \leq N$, $1 \leq k \leq N$. Using equation (39) we obtain a system of N linear equations in N unknowns (the c_j for $0 \leq j \leq N$). The number of inclusions present is simply the rank of the matrix $\mathbf{M}$ where

$$M_{k,j+1} = \phi^{(j)}(\eta_k) \quad \text{for } 0 \leq j \leq n_1 - 1, 1 \leq k \leq N. \tag{41}$$

	Computed	Actual
Radii	0.1090	0.10
	0.1532	0.15
	0.0506	0.05
Centers	$(-0.7051, -0.5034)$	$(-0.7, -0.5)$
	$(-0.0004, 0.5006)$	$(0.0, 0.5)$
	$(0.6996, -0.2497)$	$(0.7, -0.25)$

Table 1:

We then solve the system determined from (39) and use the c_j for $0 \leq j \leq n$ to construct the characteristic polynomial $p(x)$ of equation (40). The roots of this polynomial can be numerically determined to yield the values of z_j^*. Finally, we can determine A_j for $0 \leq j \leq n$ by solving the linear system

$$\sum_{j=1}^{n} A_j e^{\eta_k z_j^*} = \phi(\eta_k) \tag{42}$$

where $1 \leq k \leq N$.

4.7 Multiple Inclusion Example

In this example we again take D as the unit disk. We use three inclusions, with centers and radii as tabled below. The applied flux and other parameters are the same as the single inclusion example above.

We use an upper bound $N = 5$ on the number of blobs, and take the η_k as the Nth roots of unity. The resulting matrix $\mathbf{M}$ has singular values $0.3858, 0.1461, 0.0184$, and two singular values less than 10^{-5}. This indicates the presence of three inclusions.

With this information we now let $n = 3$ and use η_1, η_2, η_3 as the cube roots of unity, to solve for the coefficients c_0, c_1, c_2. We find characteristic equation

$$r^3 + (0.0059 + 0.2525i)r^2 + (-0.2419 - 0.1785i)r + -0.0883 + 0.3098i = 0.$$

with roots $z_1^* \approx -0.7051 - 0.5034i$, $z_2^* \approx 0.6995 - 0.2497i$, $z_3^* \approx -0.0004 + 0.5006i$, also tabulated in Table 1. We then use these estimated centers in equation (42) to solve for the A_j, and so obtain estimates $A_1 \approx -0.0004 + 0.0475i, A_2 \approx 0.0001 + 0.0102i, A_3 \approx -0.0006 + 0.0939i$. Finally, we use equation (38) to estimate the radius of each inclusion (with $u_0(x, y) = \frac{2}{\pi} y$ as before). The results are tabulated in Table 1. A graphical depiction of the actual and computed inclusions for this example is found in Figure 2.

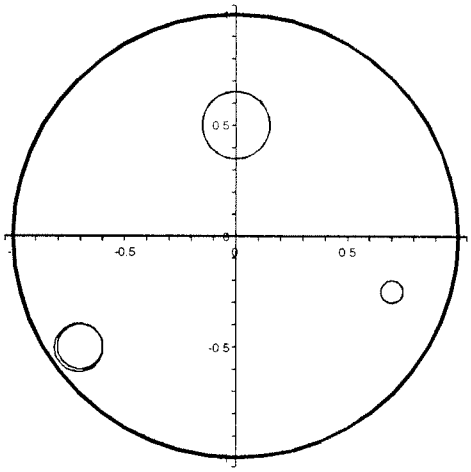

Figure 2: Detection of three inclusions on the unit disk with $s = 0$ and a flux of $g(\theta, t) = \sin(\theta)\sin(\pi t)$ for $0 \leq t \leq 1$ and $g = 0$ for $t > 1$. The data was acquired from $t = 0$ until $t = 3$.

5 The $s > 0$ Case

For $s \neq 0$, we have more freedom of choice for the input flux g on the boundary of D. Specifically, we can use any s such that the magnitude of g does not increase faster Ce^{st} for some constant C. However, we now have a slightly more complicated problem than in the $s = 0$ case.

Recall that $U_s(x, y)$ defined by equation (4) is the Laplace transform of $u(x, y, t)$, and U_s satisfies the boundary value problem (5)-(7). We will proceed as in the $s = 0$, by integrating U_s by parts against suitably chosen test functions.

5.1 The Reciprocity Gap Functional

Let w be a C^2 test function that satisfies (5) on all of D. As before an application of Green's Second Identity yields

$$RG(w) := \int_{\partial B} U_s \frac{\partial w}{\partial \mathbf{n}}\, ds = \int_{\partial D} \left(U_s \frac{\partial w}{\partial \mathbf{n}} - w \frac{\partial U_s}{\partial \mathbf{n}} \right) ds \tag{43}$$

Note that as in the $s = 0$ case we are able to compute the integral over ∂D, and thus we can compute $RG(w)$ for any w that satisfies (5).

5.2 Test Function

In what follows the Laplace parameter s is considered fixed. We use a test function w of the form

$$w(x, y) = e^{\eta_1 x + \eta_2 y} \tag{44}$$

but with $\eta_1^2 + \eta_2^2 = s$ so that w satisfies equation (5). In particular, we take

$$\begin{aligned} \eta_1 &= \sqrt{s} \cos \alpha \\ \eta_2 &= \sqrt{s} \sin \alpha \end{aligned}$$

for some fixed (possibly complex) constant α. With the parameterization $x = x^* + R\cos(\theta)$, $y = y^* + R\sin(\theta)$ of ∂B (so $\mathbf{n} =< \cos(\theta), \sin(\theta) >$) we compute $\frac{\partial w}{\partial \mathbf{n}}|_{\partial B}$ as

$$\begin{aligned} \frac{\partial w}{\partial \mathbf{n}}|_{\partial B} &= e^{\eta_1 x + \eta_2 y} \left(\eta_1 \cos\theta + \eta_2 \sin\theta \right) \\ &= \sqrt{s} e^{\sqrt{s}(\cos(\alpha)x^* + \sin(\alpha)y^*)} e^{\sqrt{s} R \cos(\theta - \alpha)} \cos(\theta - \alpha) \end{aligned} \tag{45}$$

5.3 Revised Reciprocity Gap

In what follows we will use $\phi(\alpha)$ to denote $\mathrm{RG}(w)$ with w as chosen above. We then find that

$$\begin{aligned}\phi(\alpha) &= \int_{\partial B} U_s \frac{\partial w}{\partial \mathbf{n}} \\ &= \sqrt{s} e^{\sqrt{s}(x^* \cos\alpha + y^* \sin\alpha)} \int_0^{2\pi} U_s \cos(\theta - \alpha) e^{\sqrt{s} R \cos(\theta - \alpha)}\, ds\end{aligned}$$

where $ds = R\, d\theta$. Use the 1st order Taylor approximation $e^{\sqrt{s} R \cos(\theta-\alpha)} \approx 1 + \sqrt{s} R \cos(\theta - \alpha)$ to find

$$\begin{aligned}\phi(\alpha) &\approx \sqrt{s} e^{\sqrt{s}(x^* \cos\alpha + y^* \sin\alpha)} \left(\int_0^{2\pi} U_s \cos(\theta - \alpha)\, ds + \sqrt{s} R \int_0^{2\pi} U_s \cos^2(\theta - \alpha)\, ds \right) \\ &\approx \sqrt{s} e^{\sqrt{s}(x^* \cos\alpha + y^* \sin\alpha)} \left(J_c \cos\alpha + J_S \sin\alpha + \frac{R\sqrt{s}}{2} J_0 \right) \qquad (46)\end{aligned}$$

where we denote

$$J_C = \int_0^{2\pi} U_s(R,\theta) \cos(\theta) R\, d\theta, \quad J_S = \int_0^{2\pi} U_s(R,\theta) \sin(\theta) R\, d\theta, \quad J_0 = \int_0^{2\pi} U_s(R,\theta) R\, d\theta$$

In deriving equation (46) we made use of the identity $\cos^2(x) = \frac{1}{2} + \frac{1}{2}\cos(2x)$ and we have dropped the resulting term involving $\cos(2(\theta - \alpha))$ for it does not affect $\phi(\alpha)$ too much. Specifically, a Taylor expansion of $U_s(r,\theta)$ about $r = 0$ shows that such a term will be of order R^2, and so negligible relative to the terms we've kept. For a better approximation, however, it may be of interest to keep this term and see how great the improvement is.

5.4 Finding The Center of a Single Inclusion

In order to find the center, we evaluate $\phi(\alpha)$ as given by equation (46) at five specific values for α to get five equations in five unknowns x^*, y^*, J_S, J_C, and J_0. We then numerically solve for x^* and y^* using some form of numerical solver. The variables J_S, J_C, and J_0 appear linearly, so this portion can be done in closed form; the numerical solution is necessary only to find x^* and y^*.

For our work we chose to evaluate ϕ at $\alpha = 0, \pi/4, \pi/2, \pi$, and $-\pi/2$. The equations are

thus

$$\begin{aligned}
\phi(0) &= \sqrt{s}e^{\sqrt{s}x^*}\left(J_C + \frac{R\sqrt{s}}{2}J_0\right) \\
\phi(\frac{\pi}{2}) &= \sqrt{s}e^{\sqrt{s}y^*}\left(J_S + \frac{R\sqrt{s}}{2}J_0\right) \\
\phi(\pi) &= \sqrt{s}e^{-\sqrt{s}x^*}\left(-J_C + \frac{R\sqrt{s}}{2}J_0\right) \\
\phi(-\frac{\pi}{2}) &= \sqrt{s}e^{-\sqrt{s}y^*}\left(-J_S + \frac{R\sqrt{s}}{2}J_0\right) \\
\phi(\frac{\pi}{4}) &= \sqrt{\frac{s}{2}}e^{\sqrt{\frac{s}{2}}(x^*+y^*)}\left(J_C + J_S\right)
\end{aligned}$$

5.4.1 Numerical Example

As an example, let us take D as the unit disk, B as an inclusion with center $(0.2, 0.4)$ of radius 0.2. The flux is as in previous examples, $g(\theta, t) = \sin(\theta)\sin(\pi t)$ for $0 < t < 1$, data taken on ∂D for times $0 < t < 3$. We use a Laplace parameter of $s = 2$. The data was generated in FemLab. We find estimates $x^* = 0.193, y^* = 0.400$, as well as $J_0 = 0.01705, J_C = 0.00193, J_S = 0.04182$.

As shown in the next section, the radius of the defect can be determined from J_0.

5.5 Finding the Radius of a Single Inclusion

5.5.1 The Approximate Solution to (5)-(7) for $s > 0$

We proceed in a manner very similar to the $s = 0$ case. The main difference is that the expansion of U_s via separation of variables now involves Bessel functions, rather than trig functions.

Without loss of generality, once we know where the center is we can shift our coordinate system such that $x^* = 0$ and $y^* = 0$. We use polar coordinates (r, θ) when convenient. We use the same method as before to solve (5)-(7), first letting $U_s(r, \theta) = u_0 + v_0$, where u_0 is a solution to (5) on D. The function v_0 must satisfy

$$\begin{aligned}
sv_0 - \Delta v_0 &= 0 \text{ on } D \setminus B &(47)\\
\frac{\partial v_0}{\partial \mathbf{n}} &= 0 \text{ on } \partial D &(48)\\
\frac{\partial v_0}{\partial \mathbf{n}} &= -\frac{\partial u_0}{\partial \mathbf{n}} := h(\theta) \text{ on } \partial B &(49)
\end{aligned}$$

We'll use separation of variables and let $v_0(r,\theta) = R(r)T(\theta)$. From (5) we get

$$sR(r)T(\theta) - \left[R''T + \frac{1}{r}R'T + \frac{1}{r^2}RT''\right] = 0$$

A standard separation of variables argument show that we need

$$r^2 s - \frac{r^2 R''}{R} - \frac{rR'}{R} = \frac{T''}{T} = -\lambda^2$$

for some constant λ. We end up with the following two ordinary differential equations

$$\begin{aligned} T'' + \lambda^2 T &= 0 \\ r^2 R'' + rR' - R(r^2 s + \lambda^2) &= 0 \end{aligned}$$

The solutions are

$$\begin{aligned} T(\theta) &= c_1 \cos(\lambda\theta) + c_2 \sin(\lambda\theta) \\ R(r) &= c_3 K_\lambda(\sqrt{s}r) + c_4 I_\lambda(\sqrt{s}r) \end{aligned}$$

where $I_\nu(z)$ and $K_\nu(z)$ are the modified Bessel functions of order ν of the first and second kind, respectively.

Listed below are some useful relationships where $J_\nu(z)$ and $Y_\nu(z)$ are Bessel functions of order ν of the first and second kind (see [1])

$$\begin{aligned} I_\nu(z) &= e^{\frac{\nu\iota\pi}{2}} J_\nu(ze^{-\frac{\pi\iota}{2}}) \\ K_\nu(z) &= -\frac{\pi i}{2} e^{-\frac{\nu\pi\iota}{2}} H_\nu^{(2)}(ze^{-\frac{\pi\iota}{2}}) \\ I_{\nu-1}(z) + I_{\nu+1}(z) &= 2I'_\nu(z) \\ K_{\nu-1}(z) + K_{\nu+1}(z) &= -2K'_\nu(z) \\ K_{\nu-1}(z) - K_{\nu+1}(z) &= -\frac{2\nu}{z} K_\nu(z) \\ K'_\nu(z) &= -\frac{K_{\nu-1}(z) + K_{\nu+1}(z)}{2} \\ \frac{\nu}{z} K_\nu(z) - K_{\nu+1}(z) &= K'_\nu(z) \end{aligned}$$

If we ignore the boundary condition (48) on ∂D as before and assume that D is much larger than B (so that $D \approx \mathbb{R}^2$), then we can take $c_4 = 0$ since $I_\lambda(r) \to \infty$ as $r \to \infty$, while $K_\lambda(r)$ decays rapidly (analogous to r^k versus r^{-k}). Also note that due to the continuous wrap-around condition on T, λ must be an integer which we will denote by n.

Let us use $v(r,\theta)$ to denote the resulting approximation to v_0. We can now write $v(r,\theta)$ as:

$$v(r,\theta) = \sum_{n=0}^{\infty} K_n(\sqrt{s}r)\left(a_n\cos(n\theta) + b_n\sin(n\theta)\right)$$

and also

$$\frac{\partial K_n(\sqrt{s}r)}{\partial r} = \frac{nK_n(\sqrt{s}r)}{r} - \sqrt{s}K_{n+1}(\sqrt{s}r)$$

Computing the normal derivative $\frac{\partial v}{\partial r}$ and evaluating at $r = R$ in order to apply the Neumann data yields

$$v_r(R,\theta) = \sum_{n=0}^{\infty}\left(\frac{nK_n(\sqrt{s}R)}{R} - \sqrt{s}K_{n+1}(\sqrt{s}R)\right)\left(a_n\cos(n\theta) + b_n\sin(n\theta)\right) = h(\theta).$$

We can compute the coefficients a_n and b_n by viewing $v_r(R,\theta)$ as a Fourier series expansion of $h(\theta)$. We obtain

$$\begin{aligned}\left(\frac{nK_n(\sqrt{s}R)}{R} - \sqrt{s}K_{n+1}(\sqrt{s}R)\right)a_n &= \frac{1}{\pi}\int_0^{2\pi} h(\theta)\cos(n\theta)\,d\theta \\ \left(\frac{nK_n(\sqrt{s}R)}{R} - \sqrt{s}K_{n+1}(\sqrt{s}R)\right)b_n &= \frac{1}{\pi}\int_0^{2\pi} h(\theta)\sin(n\theta)\,d\theta\end{aligned}$$

After simplification we have

$$\begin{aligned}a_n &= \frac{1}{\pi}\frac{1}{\frac{nK_n(\sqrt{s}R)}{R} - \sqrt{s}K_{n+1}(\sqrt{s}R)}\int_0^{2\pi} h(\theta)\cos(n\theta)\,d\theta \\ b_n &= \frac{1}{\pi}\frac{1}{\frac{nK_n(\sqrt{s}R)}{R} - \sqrt{s}K_{n+1}(\sqrt{s}R)}\int_0^{2\pi} h(\theta)\sin(n\theta)\,d\theta\end{aligned}$$

For this computation, we used a slightly less accurate approximation of $\phi(\alpha)$ as listed below. Specifically, we used the zeroth order Taylor approximation $e^{\sqrt{s}R\cos(\theta-\alpha)} \approx 1$. In this case we find

$$\begin{aligned}\phi(\alpha) &\approx \sqrt{s}e^{\sqrt{s}(x^*\cos\alpha + y^*\sin\alpha)}\int_0^{2\pi} U_s\cos(\theta-\alpha)\,ds \\ &= \sqrt{s}e^{\sqrt{s}(x^*\cos\alpha + y^*\sin\alpha)}\left(J_C\cos\alpha + J_S\sin\alpha\right)\end{aligned}$$

with J_C and J_S as defined above. We now substitute $U_s = u_0 + v$, and define the quantity J as

$$J = \sqrt{s}(J_C\cos\alpha + J_S\sin\alpha) \tag{50}$$

so that

$$\phi(\alpha) \approx Je^{\sqrt{s}(x^*\cos\alpha + y^*\sin\alpha)}. \tag{51}$$

Note that after we know the center (x^*, y^*), we can recover J.

In expanded form, we have (recall $\eta_1 = \sqrt{s}\cos(\alpha), \eta_2 = \sqrt{s}\sin(\alpha)$)

$$J = \int_{\partial B} [\eta_1 \cos\theta + \eta_2 \sin\theta]\, u\, ds = \int_0^{2\pi} [\eta_1 \cos\theta + \eta_2 \sin\theta]\, (u_0(R,\theta) + v(R,\theta)) R\, d\theta \qquad (52)$$

The portion of (52) involving u_0 can be approximated in the same way as the $s = 0$ case. To restate, $u_0|_{\partial B} = u_0(z^*) + \nabla u_0(z^*) \cdot < R\cos(\theta), R\sin(\theta) > + O(R^2)$. This is just a first order Taylor series approximation of u_0 about the point z^*, which is in our case, the origin.

To analyze the second part of (52) we compute by using the following small-r Bessel function approximations (again, see [1])

$$K_m(r) \approx \begin{cases} \log r & m = 0 \\ \frac{1}{2}(m-1)!(\frac{1}{2}r)^{-m} & m \neq 0 \end{cases}$$

To lowest order we need only consider K_1 and K_2 (terms involving other K_n will drop out below, due to orthogonality considerations), which are specifically

$$\begin{aligned} K_1(r) &\approx \frac{1}{2}\frac{2}{r} = \frac{1}{r} \\ K_2(r) &\approx \frac{1}{2}(\frac{1}{2}r)^{-2} = \frac{1}{2}\frac{4}{r^2} = \frac{2}{r^2} \end{aligned}$$

A bit of computation and approximation then shows that

$$
\begin{aligned}
J &\approx \int_0^{2\pi} [\eta_1 \cos\theta + \eta_2 \sin\theta] \left(u_0(z^*) + \frac{\partial u_0}{\partial x}(z^*) R\cos\theta + \frac{\partial u_0}{\partial y}(z^*) R\sin\theta \right) R\, d\theta \\
&\quad + \int_0^{2\pi} [\eta_1 \cos\theta + \eta_2 \sin\theta]\, v(R,\theta) R\, d\theta \\
&= \frac{\partial u_0}{\partial x}(z^*) R^2 \eta_1 \int_0^{2\pi} \cos^2\theta\, d\theta + \frac{\partial u_0}{\partial y}(z^*) R^2 \eta_2 \int_0^{2\pi} \sin^2\theta\, d\theta \\
&\quad + \int_0^{2\pi} [\eta_1 \cos\theta + \eta_2 \sin\theta]\, v(R,\theta) R\, d\theta \\
&= \frac{\partial u_0}{\partial x}(z^*) R^2 \eta_1 \pi + \frac{\partial u_0}{\partial y}(z^*) R^2 \eta_2 \pi + \int_0^{2\pi} [\eta_1 \cos\theta + \eta_2 \sin\theta]\, v(R,\theta) R\, d\theta \\
&= R^2 \pi \nabla u_0(z^*) \cdot < \eta_1, \eta_2 > + R \int_0^{2\pi} [\eta_1 \cos\theta + \eta_2 \sin\theta] \sum_{n=0}^{\infty} K_n(\sqrt{s}R) \left[a_n \cos(n\theta) + b_n \sin(n\theta) \right] d\theta \\
&= R^2 \pi \nabla u_0(z^*) \cdot < \eta_1, \eta_2 > + R\eta_1 \int_0^{2\pi} K_1(\sqrt{s}R) a_1 \cos^2\theta\, d\theta + R\eta_2 \int_0^{2\pi} K_1(\sqrt{s}R) b_1 \sin^2\theta\, d\theta \\
&\approx R^2 \pi \nabla u_0(z^*) \cdot < \eta_1, i\eta_2 > + R\eta_1 \pi \frac{1}{\sqrt{s}R} a_1 + R\pi\eta_2 \frac{1}{\sqrt{s}R} b_1 \\
&= R^2 \pi \nabla u_0(z^*) \cdot < \eta_1, i\eta_2 > \\
&\quad + \frac{\pi}{\sqrt{s}} \left(\eta_1 \int_0^{2\pi} h(\theta)\cos(\theta)\, d\theta + \eta_2 \int_0^{2\pi} h(\theta)\sin(\theta)\, d\theta \right) \frac{1}{\pi} \frac{1}{\frac{K_1(\sqrt{s}R)}{R} - \sqrt{s} K_2(\sqrt{s}R)} \\
&\approx R^2 \pi \nabla u_0(z^*) \cdot < \eta_1, i\eta_2 > + \frac{\pi}{\sqrt{s}} \left(\eta_1 \int_0^{2\pi} h(\theta)\cos(\theta)\, d\theta + \eta_2 \int_0^{2\pi} h(\theta)\sin(\theta)\, d\theta \right) \left(-\frac{\sqrt{s}R^2}{\pi} \right) \\
&= R^2 \pi \nabla u_0(z^*) \cdot < \eta_1, i\eta_2 > - R^2 \left(\eta_1 \int_0^{2\pi} h(\theta)\cos(\theta)\, d\theta + \eta_2 \int_0^{2\pi} h(\theta)\sin(\theta)\, d\theta \right)
\end{aligned}
$$

We now use an additional approximation that $h(\theta) = -\frac{\partial u_0}{\partial r} = -\nabla u_0 \cdot < \cos(\theta), \sin(\theta) > \approx -\nabla u_0(z^*) \cdot < \cos(\theta), \sin(\theta) >$. Applying this yields

$$
\begin{aligned}
J &= R^2 \pi \nabla u_0(z^*) \cdot < \eta_1, \eta_2 > - R^2 \eta_1 \int_0^{2\pi} \left[-\frac{\partial u_0}{\partial x}(z^*)\cos\theta - \frac{\partial u_0}{\partial y}(z^*)\sin\theta \right] \cos\theta\, d\theta \\
&\quad - R^2 \eta_2 \int_0^{2\pi} \left[-\frac{\partial u_0}{\partial x}(z^*)\cos\theta - \frac{\partial u_0}{\partial y}(z^*)\sin\theta \right] \sin(\theta)\, d\theta \\
&= R^2 \pi \nabla u_0(z^*) \cdot < \eta_1, \eta_2 > + R^2 \eta_1 \frac{\partial u_0}{\partial x}(z^*)\pi + R^2 \eta_2 \frac{\partial u_0}{\partial y}(z^*)\pi \\
&= 2\pi R^2 \nabla u_0(z^*) \cdot < \eta_1, \eta_2 > \\
&= 2\pi \sqrt{s} R^2 \nabla u_0(z^*) \cdot < \cos(\alpha), \sin(\alpha) > \qquad (53)
\end{aligned}
$$

	Computed	Actual
Radius	0.197	0.20
Center	(0.201888, 0.401673)	(0.20, 0.40)

Table 2:

5.6 Example: Find the Radius

For this computation we use the same parameters as in section 5.4.1, including Laplace parameter $s = 2$. We have already identified the center. We find from the same data (using $\alpha = \pi/2$) that $J \approx 0.04182$. We also need to know u_0. In this case an expansion in Bessel functions in polar coordinates about the origin shows that

$$u_0(r, \theta) \approx 0.1955 \frac{I_1(r\sqrt{2})}{r}.$$

Finally, we use equation (53) to find estimate $R \approx 0.197$, remarkably accurate.

Results are listed in Table 2.

6 Conclusion and Future Work

We have used the Laplace Transform in order to eliminate t from the time dependent problem where some collection of circular inclusions, which completely block heat flow, are contained in some two-dimensional region D. Yet to be discovered is a method for extracting the radii and centers of multiple inclusions in the s nonzero case. Ideally, there is a nice way to solve this problem, although with just one inclusion we had to resort to a rather crude approach - solving a system of equations numerically - though the system contained only two equations and no solves of the forward problem are needed.

Beyond the multiple inclusion, s nonzero case, it would be interesting to try and modify our model so that partial heat flow can occur over the boundary of each inclusion. Thus, we would have a boundary condition of the form $\frac{\partial u}{\partial \mathbf{n}} = k[u]$ on ∂B.

Finally, it would be prudent to look into the 3-dimensional analog of our problem - that is, some arbitrary solid blob with a spherical hole inside with neither radius nor center known.

References

[1] Abramowitz, M., and Stegun, I., Handbook of Mathematical Functions, Dover, 1965.

[2] Andrieux, S., and Ben Abda, A., Identification de fissures planes par une donne de bord unique; un procd direct de localisation et didentification, C.R. Acad. Sci.. Paris I, 1992, 315, pp. 1323-1328.

[3] Bryan, K., Krieger, R., Trainor, N., Imaging of Multiple Linear Cracaks Using Impedance Data.

[4] McQuarrie, Donald A., Mathematical Methods for Scientists and Engineers.

[5] Christian N., Johnson M., Non-Destructive Testing of Thermal Resistances for a Single Inclusion in a 2-Dimensional Domain.

[6] Bryan, K., An Inverse Problem in Non-Destructive Testing: The "Reciprocity Gap" Approach.